Leslie, A. G. W., Arnoff, S., Chandrasekaran, R., & Ratliff, R. L. (1980) *J. Mol. Biol. 143*, 49–72.
Lundgren, S., Ronne, H., Rask, L., & Peterson, P. A. (1984) *J. Biol. Chem. 259*, 7780–7784.
Maniatis, T., Fritsch, E. F., & Sambrook, J., Eds. (1982) in *Molecular Cloning: A Laboratory Manual*, pp 383–389, Cold Spring Harbor Laboratory, Cold Spring Harbor, NY.
Mason, A. J., Evans, B. A., Cox, D. R., Shine, J., & Richards, R. I. (1983) *Nature (London) 303*, 300–307.
Messing, J. (1983) *Methods Enzymol. 101*, 20–78.
Mirkin, S. M., Lyamichev, V. I., Drushlyak, K. N., Dorbrynin, Y. N., Filippov, S. A., & Frank-Kamenetskii, M. D. (1987) *Nature (London) 330*, 495–497.
Mount, S. M. (1982) *Nucleic Acids Res. 10*, 459–472.
Proudfoot, N. J., & Brownlee, G. G. (1976) *Nature (London) 263*, 211–214.
Sanger, F., Nicklen, S., & Coulson, A. (1977) *Proc. Natl. Acad. Sci. U.S.A. 74*, 5463–5467.
Schachter, M. (1963) *Ann. N.Y. Acad. Sci. 104*, 108–115.
Schreir, P. H., & Cortese, R. (1979) *J. Mol. Biol. 129*, 169–172.
Schedlich, L. J., Bennetts, B. H., & Morris, B. J. (1987) *DNA 6*, 429–437.
Seidah, N. G., Chen, J. S. D., Mardini, G., Benjannet, S., Chretin, M., Boucher, R., & Genest, J. (1979a) *Biochem. Biophys. Res. Commun. 86*, 1002–1013.
Seidah, N. G., Chan, J. S. D., Routhier, R., Gossard, F., Chretien, M., Boucher, R., & Genest, J. (1979b) in *Peptides* (Gross, E., & Meienhofer, J., Eds.) pp 921–924, Pierce Chemical Co., Rockford, IL.
Sen, D. G., & Gilbert, W. (1988) *Nature (London) 334*, 364–366.
Shih, H. C., Chao, L., & Chao, J. (1986) *Biochem. J. 238*, 145–149.
Singleton, C. K., Klysik, J., Stirdivant, S. M., & Wells, R. D. (1982) *Nature (London) 299*, 312–316.
Stringer, J. R. (1985) *Mol. Cell. Biol. 5*, 1247–1259.
Swift, G. H., Dagorn, J.-C., Ashley, P. L., Cummings, S. W., & MacDonald, R. J. (1982) *Proc. Natl. Acad. Sci. U.S.A. 79*, 7263–7267.
Thomas, K. A., Baglan, N. C., & Bradshaw, R. A. (1981) *J. Biol. Chem. 256*, 9156–9166.
Weinreb, A., Katzenberg, D. R., Gilmore, G. L., & Birshtein, B. K. (1988) *Proc. Natl. Acad. Sci. U.S.A. 85*, 529–533.

Kinetic and Structural Effects of Activation of Bovine Kidney Aldose Reductase†

C. E. Grimshaw,* M. Shahbaz, G. Jahangiri, C. G. Putney, S. R. McKercher, and E. J. Mathur‡

Division of Biochemistry, Division of Preclinical Neuroscience and Endocrinology, Department of Molecular and Experimental Medicine, Research Institute of Scripps Clinic, Scripps Clinic and Research Foundation, La Jolla, California 92037

Received October 20, 1988; Revised Manuscript Received March 16, 1989

ABSTRACT: Aldose reductase, purified to homogeneity from bovine kidney, is converted in a temperature-dependent process from a low-K_m/low-V_{max} form to a high-K_m/high-V_{max} form of the enzyme. Activation, which results in significant changes in the protein secondary structure, as detected by fluorescence spectroscopy, circular dichroism, and thiol modification with 5,5′-dithiobis(2-nitrobenzoic acid), has no effect on the apparent M_r, pI, or homogeneity of the enzyme, as judged by sodium dodecyl sulfate–polyacrylamide gel electrophoresis and agarose isoelectric focusing. V_{max}, which varied less than 3-fold for a series of aldehyde substrates with either activation state of the enzyme, increased an average of (17 ± 4)-fold upon activation of the enzyme. $V/K_{aldehyde}$ increased or decreased up to 4-fold, depending on the substrate. Activation desensitized the enzyme to inhibition by aldose reductase inhibitors, with the apparent K_i value increasing from 2-fold for Epalrestat [ONO-2235, (*E*)-3-(carboxymethyl)-(*E*)-5-[2-methyl-3-phenylpropenylidene]-rhodanine] to 200-fold for AL-1576 (spiro[2,7-difluorofluorene-9,4′-imidazolidine]-2′,5′-dione). Biphasic double-reciprocal plots for the aldehyde substrates and biphasic Dixon plots for inhibition by AL-1576 and Statil [ICI-128 436; 3-[(4-bromo-2-fluorobenzyl)-4-oxo-3*H*-phthalazin-1-ylacetic acid], observed during the course of activation, are quantitatively accounted for by the individual contributions of the two enzyme forms. On the basis of an analysis of the kinetic data, a mechanism is proposed in which isomerization of the free enzyme limits the rate of the forward reaction for the unactivated enzyme and is the primary step affected by activation.

Aldose reductase (ALR2;[1] alditol:NADP$^+$ 1-oxidoreductase; EC 1.1.1.21; also referred to as "low-K_m" aldehyde reductase) catalyzes the NADPH-dependent reduction of a wide variety of aldehydes to the corresponding alcohols:

$$NADPH + RCHO + H^+ \leftrightarrow NADP^+ + RCH_2OH$$

The kinetic properties of this reaction have been a subject of controversy, with conflicting reports of either Michaelis–Menten type kinetics (Boghosian & McGuinness, 1979; Wermuth et al., 1982; Branlant, 1982; Hara et al., 1983; Cromlish & Flynn, 1983a,b; Morjana & Flynn, 1989) or nonlinear double-reciprocal plots displaying apparent negative

† This work was supported by a grant to C.E.G. from the NIH (DK 32218) and the Olive H. Whittier Fund. Support for the VAX 11/750 in the General Clinical Research Center, Scripps Clinic and Research Foundation, was provided by a Division of Research Resources Grant (RR 00833) from the NIH. This is Publication No. 5211 BCR from the Research Institute of Scripps Clinic, Scripps Clinic and Research Foundation.

* Address correspondence to this author.
‡ Present address: Stratagene Cloning Systems, La Jolla, CA 92037.

0006-2960/89/0428-5343$01.50/0

cooperativity for the nucleotide and certain aldehyde substrates (Håstein & Velle, 1969; Sheaff & Doughty, 1976; Hoffman et al., 1980; Daly & Mantle, 1982; Conrad & Doughty, 1982; Halder & Crabbe, 1984; Srivastava et al., 1985; Poulsom, 1986). Originally, the nonlinear kinetic behavior was attributed to the presence of more than one enzyme catalyzing the same reaction (Turner & Tipton, 1972; Whittle & Turner, 1981; Cromlish & Flynn, 1983a), a hypothesis supported by the subsequent identification of at least four distinct NADPH-dependent aldo–keto reductases in tissues such as brain and kidney (Hoffman et al., 1980; Daly & Mantle, 1982; Hara et al., 1983; Cromlish et al., 1985). These monomeric reductases are similar with respect to molecular mass and preference for NADPH as the nucleotide cofactor and have overlapping specificity for the aldehyde substrate [reviewed in Flynn (1982a,b) and Wermuth (1985)]. However, it was suggested, on the basis of a detailed study of a homogeneous preparation of the bovine lens enzyme, that the nonlinear kinetics are an intrinsic property of the ALR2 mechanism (Sheaff & Doughty, 1976; Doughty & Conrad, 1982). Interpretation of the kinetic data has been further complicated by the observation of microheterogeneity in purified preparations of aldose reductase (Jedziniak & Kinoshita, 1971; Gabbay & Cathcart, 1974; Wermuth et al., 1982; Cromlish & Flynn, 1983a; Tanimoto et al., 1983).

Several alternative explanations for the nonlinear kinetic results have been proposed. Substrate activation of the type described by Dalziel and Dickinson (1966) for oxidation of secondary alcohols by horse liver alcohol dehydrogenase has been observed for ALR2 isolated from *Rhodotorula* (Sheys & Doughty, 1971). Apparent negative cooperativity could also arise if more than one form of the substrate were catalytically active, such as the free carbonyl species and the hydrate (or thiohemiacetal, when thiols are present).

ALR2 is of clinical interest because of the postulated role for this enzyme in the etiology of diabetic complications, including nephropathy, peripheral neuropathy, retinopathy, and sugar cataract (Kador & Kinoshita, 1985; Dvornik, 1987a). As a result, a substantial effort has been made to develop compounds specifically targeted as ALR2 inhibitors (ARIs) (Kador et al., 1985; Dvornik, 1987b). In vitro testing of commercial ARIs has also been controversial. Thus, significant differences in ARI potency have been reported for preparations of ALR2 obtained from different species (Kador et al., 1980; Dvornik, 1987b; Poulsom, 1987), from different tissues of the same species (Kador et al., 1980), and even during purification of the enzyme (Kador et al., 1983; Maragoudakis et al., 1984). Other studies, however, have found little difference in ARI potency (Muller et al., 1985; Griffin et al., 1987) and a similarity in physical, chemical, and kinetic properties for ALR2 isolated from several species of mammalian lens (Conrad & Doughty, 1982). The possibility of a correlation between the nonlinear kinetic properties of the ALR2 reaction with the differences in ARI potency has not been evaluated.

The present study was initiated to determine the cause of the nonlinear kinetics observed with ALR2. To this end, we have purified ALR2 to homogeneity from bovine kidney and have characterized the physical and kinetic properties of the enzyme. In this paper, we present evidence for a novel conversion of the initially isolated, low-K_m/low-V_{max} form of the enzyme to an activated, high-K_m/high-V_{max} form. We further show that the separate contributions of the two enzyme forms quantitatively account for the biphasic double-reciprocal plots observed during the course of the activation process and that activation is accompanied by significant changes in the protein secondary structure and in the binding of various ARIs. Kinetic analysis indicates that isomerization of the free enzyme, which limits the rate of the forward reaction in the unactivated enzyme, is the primary step affected by activation. The consequences of these results for the modulation of ALR2 activity in vitro and in vivo are discussed. Portions of this study have been presented previously (Grimshaw & Mathur, 1984; McKercher et al., 1985; Grimshaw et al., 1988).

Experimental Procedures

Materials. The following were obtained from the indicated commercial sources: Sephadex G-75 (Pharmacia); Trisacryl GF-05 and DEAE-Trisacryl M (LKB); enzyme grade ammonium sulfate (Schwarz-Mann); valproic acid (Saber Laboratories); $NADP^+$ and NADPH (Boehringer-Mannheim); Bio-Gel HTP hydroxyapatite, reagents for polyacrylamide gel electrophoresis, and pH 3–10 ampholytes (Bio-Rad); IsoGel agarose, Gelbond, and protein standards for isoelectric focusing (FMC Marine Colloids Division); pH 4.5–5.0 ampholytes (Serva); reactive red 120 agarose, 5,5′-dithiobis(2-nitrobenzoic acid) (DTNB), aldehyde substrates, protein standards for SDS–PAGE, and other chemicals and biochemicals (Sigma). Sorbinil (Pfizer Pharmaceutical Co.), Tolrestat (Ayerst Laboratories), AL-1576 (Alcon Laboratories), Epalrestat (ONO, Ltd.), and Statil (ICI Pharmaceuticals Group, Stuart Pharmaceuticals) were generously provided by the companies indicated. Solutions were prepared with distilled, deionized water that had been treated with Chelex 100 (Na^+ form) to remove trace metal ion contaminants. pH was measured with a Radiometer Model PHM 84 pH meter and GKC-2321C combined electrode.

Standard Enzyme Activity Assay. During the purification procedure, bovine kidney ALR2 was routinely assayed by measuring, with a Beckman DU monochromator, Gilford 252 optical density convertor, and Linseis 2025 strip chart recorder, the rate of enzyme-dependent decrease in the absorbance at 340 nm [ϵ = 6220 M^{-1} cm^{-1} (P-L Biochemicals, 1961)]. Assays were conducted at 25 °C in 1.0 cm path length quartz cuvettes containing 5 mM DL-glyceraldehyde and 160 μM NADPH in a final volume of 1.0 mL of buffer containing 100 mM sodium phosphate, 0.1 mM dithiothreitol, and 0.1 mM Na_2EDTA, pH 7.2. Temperature was maintained to within ±0.1 °C with a thermostated circulating water bath and thermospacers. One unit of activity corresponds to 1 μmol of product/min, and specific activity is expressed as units per milligram of protein. During the purification procedure, protein concentration was determined by the dye-binding method of Bradford (1976) using bovine serum albumin as the standard. The concentration of purified ALR2 was determined by fluorometric titration of the $NADP^+$/NADPH binding sites (see below).

[1] Abbreviations: ARI, aldose reductase inhibitor; Na_2EDTA, disodium ethylenediaminetetraacetate; DEAE, diethylaminoethyl; DTNB, 5,5′-dithiobis(2-nitrobenzoic acid); Mops, 3-(*N*-morpholino)propanesulfonic acid; SDS, sodium dodecylsulfate; SDS–PAGE, sodium dodecyl sulfate–polyacrylamide gel electrophoresis; NADPH, reduced β-nicotinamide adenine dinucleotide phosphate; $NADP^+$, oxidized β-nicotinamide adenine dinucleotide phosphate; Epalrestat (ONO-2235), (*E*)-3-(carboxymethyl)-(*E*)-5-[2-methyl-3-phenylpropenylidene]rhodanine; Tolrestat (AY-27 773), *N*-[[5-(trifluoromethyl)-6-methoxy-1-naphthalenyl]thioxomethyl]-*N*-methylglycine; Sorbinil (CP-45 634), (*S*)-2,3-dihydro-6-fluorospiro[4*H*-1-benzopyran-4,4′-imidazolidine]-2′,5′-dione; AL-1576, spiro[2,7-difluorofluorene-9,4′-imidazolidine]-2′,5′-dione; Statil (ICI-128 436), 3-[(4-bromo-2-fluorobenzyl)-4-oxo-3*H*-phthalazin-1-ylacetic acid. The nomenclature for aldose reductase (ALR2) was recommended by the First International Workshop on Aldehyde Dehydrogenase and Aldehyde Reductase, held in Bern, Switzerland, on July 12–14, 1982 (Turner & Flynn, 1982).

Kinetic Studies. For initial velocity studies, assays were conducted in MOPSED buffer (50 mM Mops, 0.1 mM Na_2EDTA, and 0.1 mM dithiothreitol, pH 7.0) containing the indicated concentrations of NADPH, aldehyde, and inhibitor or activator. Initial rates at saturating NADPH (160 μM) were measured by monitoring the absorbance decrease at 340 nm as described above. For NADPH concentrations in the 1–10 μM range, the initial rates were determined by measuring, with a Perkin-Elmer 650-40 spectrofluorometer, Xe light source, and Hitachi 057 X-Y recorder, the rate of enzyme-dependent decrease in NADPH fluorescence (excitation at 340 nm; emission at 460 nm). Assays were conducted in 1.0-cm^2 quartz cuvettes in a final volume of 1.0 mL. The full-scale deflection was calibrated to equal a 1 μM change in NADPH concentration. For all assays, initial rates were corrected for the rate of absorbance decrease detected in the absence of the aldehyde substrate (at most, $\leq$5%). Inhibition by ALR2 inhibitors was determined at a saturating level of both substrates (10 mM glycolaldehyde, 160 μM NADPH) by two methods: (1) For tight-binding inhibition; initial velocity, measured as a function of enzyme concentration at several fixed levels (including zero) of inhibitor, was plotted versus [enzyme] (Williams & Morrison, 1979). (2) For simple inhibition, (initial velocity)$^{-1}$, measured as a function of inhibitor concentration, was plotted versus [inhibitor] (Dixon, 1953). The concentrations of inhibitors were determined in 5 mM Mops buffer (pH 7.0) by using the indicated extinction coefficients: Tolrestat (ϵ_{272nm} = 9370 M^{-1} cm^{-1}; Dushan Dvornik, personal communication); AL-1576 (ϵ_{265nm} = 13400 M^{-1} cm^{-1}; Brenda W. Griffin, personal communication); Sorbinil (ϵ_{284nm} = 3100 M^{-1} cm^{-1}; Nancy J. Hutson, personal communication); and Statil (ϵ_{275nm} = 8260 M^{-1} cm^{-1}; determined by using a formula weight of 390.2 g/mol).

Fluorescence Titration. The dissociation constants (K_d) for binary E·nucleotide complexes were determined from the quenching of protein fluorescence upon nucleotide binding (excitation at 285 nm; emission at 340 nm). Titrations were carried out by serial addition of aliquots (2 μL) of a concentrated stock solution of ligand to a 1.0-cm^2 quartz semimicrocuvette containing ALR2 in MOPSED buffer. The titration of a standard glycyl–tryptophan solution under identical conditions was used to correct for inner filter effects. Equilibrium fluorescence readings were recorded 3 min after the addition of ligand, and the K_d and number of binding sites were estimated by least-squares analysis using (Stinson & Holbrook, 1973)

$$[L_t]/\Phi = K_d(1 - \Phi)^{-1} + p[E_t] \quad (1)$$

where $[L_t]$ and $[E_t]$ are the total concentrations of ligand and enzyme, respectively, p is the number of independent and equivalent binding sites on E, and Φ is the ratio of the observed fluorescence change to the maximum fluorescence change ($\Phi = \Delta F/\Delta F_{max}$). For ALR2, p was calculated to be 1.0. Enzyme and ligand concentrations were adjusted for optimal determination of both K_d and $[E_t]$. The upper limit for K_d that could be determined by this method was 50 nM.

Chemical Modification of Enzyme Thiol Groups. The number and reactivity of the enzyme's cysteine sulfhydryl groups were determined by reaction with DTNB at 25 °C using a modification of the method of Riddles et al. (1983). For the nondenatured enzyme sample, exogenous thiol was removed by rapid gel filtration through a column (1.0 × 12 cm) of Trisacryl GF-05 resin equilibrated with buffer (100 mM sodium phosphate and 1 mM Na_2EDTA, pH 7.27) that had been degassed and purged with argon. The time course of thiol modification was continuously monitored as the increase in absorbance at 412 nm (ϵ = 14150 M^{-1} cm^{-1}); the reference cell contained everything except enzyme. Aliquots (50 μL) were removed from an identical, but separate, sample at various times during the course of the DTNB reaction, and the remaining enzyme activity was determined by using the standard assay protocol. For the denatured sample, the enzyme was incubated, after buffer exchange by gel filtration, at 37 °C for 30 min in buffer containing 1% (w/v) SDS, prior to reaction with DTNB in the same buffer. For determination of the total number of cysteine sulfhydryl groups, the enzyme was first denatured in 1% (w/v) SDS and then reduced with excess dithiothreitol. Exogenous thiol was removed by gel filtration with buffer containing 1% (w/v) SDS, and the DTNB reaction was conducted as before.

Circular Dichroism Measurements. Circular dichroism was measured with a computer-controlled AVIV 61DS spectropolarimeter under constant nitrogen flush at 25.0 °C. The instrument had been calibrated with *d*-10-camphorsulfonic acid (Cassim & Yang, 1969). Enzyme samples were exchanged into 20 mM sodium phosphate buffer (pH 7.2) containing 0.1 mM Na_2EDTA by rapid gel filtration (Trisacryl GF-05) and were degassed under nitrogen before use. Enzyme concentrations (15–45 μg/mL) were determined by fluorescence titration of $NADP^+$ binding sites, as described above. Digitized spectra were recorded in triplicate over the region 185–350 nm by using a 0.1 cm path length quartz cuvette. Data were collected by a microcomputer at a scan rate of 7.5 nm/min with an interval of 0.25 nm and a fixed bandwidth of 0.5 nm. The averaged spectrum was smoothed by using the nonlinear regression and statistical analysis software provided by the manufacturer. Mean residue ellipticities, $[\Theta]$ (expressed as deg cm^2 $dmol^{-1}$), were calculated by using

$$[\Theta] = ([\Theta]_{obs} \times 100MRW)/(lc) \quad (2)$$

where $[\Theta]_{obs}$ is the observed ellipticity (deg), MRW is the mean residue molecular weight [calculated from the amino acid composition (Doughty et al., 1988) to be 114], l is the optical pathlength (cm), and c is the protein concentration (mg/mL). The digitized enzyme spectra over the region 190–240 nm, corrected by subtraction of the similarly processed spectrum for the buffer blank, were analyzed to determine the relative proportions of α-helix, β-sheet, β-turn, and random coil by using the multiple linear regression program supplied by AVIV. This program is a protein secondary structure estimator that is similar to the unconstrained multiple linear regression program described by Yang et al. (1986) and which utilizes the reference spectra of Dr. J. T. Yang (Chang et al., 1978).

Data Processing. Reciprocal initial velocities were plotted vs reciprocal substrate concentrations, and the experimental data were fitted by the least-squares method, assuming equal variance (constant absolute error) for the v_i values (Wilkinson, 1951), using the FORTRAN programs of Cleland (1979). When the range of experimental velocities was a power of 10 or more, a constant proportional error was assumed and the v_i values were fit to the appropriate equation expressed in log form (e.g., eq 5 and 11, and the log form of eq 3, 4, and 7).

$$v_i = VA/(K_a + A) \quad (3)$$

$$v_i = VA/(K_a + A + A^2/K_1) \quad (4)$$

$$\log v_i = \log [V(A^2 + dA)/(A^2 + bA + c)] \quad (5)$$

$$v_i = [V_1A/(K_{a1} + A)] + [V_2A/(K_{a2} + A)] \quad (6)$$

$$v_i = VAB/(AB + K_aB + K_bA + K_{ia}K_b) \quad (7)$$

$$v_i = VA/[K_a(1 + I/K_{is}) + A(1 + I/K_{ii})] \quad (8)$$

$$v_i = V/(1 + I/K_i) \quad (9)$$

$$v_i = [V_1/(1 + I/K_{i1})] + [V_2/(1 + I/K_{i2})] \quad (10)$$

$$\log v_i = \log \{(V/2)[pE_t - I_t - K_i + [(K_i + pE_t - I_t)^2 + 4K_iI_t]^{1/2}]\} \quad (11)$$

The points in the figures are the experimentally determined values, while the curves are calculated from fits of these data to the appropriate equation. Linear double-reciprocal plots were fitted to eq 3, and eq 4 was used when substrate inhibition was observed. When apparent negative cooperativity was observed, the data were fitted to eq 5, where $1/V = 1/(V_1 + V_2)$ is the reciprocal of the intercept at the ordinate, and b–d are combinations of the kinetic parameters derived by rearrangement of eq 6, which describes the net velocity when there are two enzymes present that can catalyze the same reaction (Segel, 1975). Equation 7 describes an intersecting initial velocity pattern, where K_a and K_b are the Michaelis constants for A and B, respectively, K_{ia} is the apparent dissociation constant for A, and V is the maximum velocity. Data conforming to linear noncompetitive inhibition were fitted to eq 8, where K_{is} and K_{ii} are the slope and intercept inhibition constants, respectively. Inhibition data were fitted to eq 9 for determination of K_i at a saturating level of both substrates. Inhibition data corresponding to a biphasic Dixon plot [$1/v_i$ versus [I] (Dixon, 1953)] were fitted to eq 5, where b–d are combinations of the K_i and V values for the two enzyme forms, derived by rearrangement of eq 10. Data conforming to tight-binding inhibition were fitted to eq 11, where p is the number of active sites, E_t is the concentration of enzyme, I_t is the inhibitor concentration, and K_i is the apparent inhibition constant (Blanchard & Cleland, 1980). The kinetic nomenclature used is that of Cleland (1963).

Gel Electrophoresis and Isoelectric Focusing. Samples were analyzed by SDS–PAGE in 11% polyacrylamide gels by using a modification of the method of Laemmli (1970); the modified 2× sample application buffer containing 1 mM Na_2EDTA and 50 mM dithiothreitol was used in place of 2-mercaptoethanol, and samples were boiled for only 60 s. Protein was detected with silver stain (Bio-Rad Bulletin 1089, Bio-Rad Laboratories). Horizontal isoelectric focusing in 1 mm agarose slab gels was performed by using an LKB Multiphor II at 12 °C. Agarose gels were cast on Gelbond sheets (Saravis & Zamcheck, 1979) by using IsoGel agarose containing 5 mM dithiothreitol and 2.0% (w/v) of pH 4.5–5 (Serva) and 0.5% (w/v) of pH 3–10 (Bio-Rad) ampholytes. Protein bands were detected with silver stain (Willoughby & Lambert, 1983). The following protein standards (FMC Marine Colloids Division) were used to establish the pI scale: amyloglucosidase (pI = 3.6), glucose oxidase (pI = 4.2), ovalbumin (pI = 4.8), β-lactoglobin (pI = 5.4, 5.5), and carbonic anhydrase (pI = 6.1).

Immunoquantitation of ALR2. The amount of ALR2 obtained after each step of the purification procedure was determined by soft-laser scanning densitometry of autoradiographs of Western blots probed with a monospecific, polyclonal anti-bovine kidney ALR2 antiserum and ^{125}I-labeled protein A, as described elsewhere (Mathur & Grimshaw, 1986).

Purification of Bovine Kidney ALR2. Step 1: Tissue Homogenate. All steps were performed at 4 °C. Fresh bovine kidney medulla (900 g) (fat and cortical tissue were removed) was homogenized for 40 s in a 4 L capacity Waring blendor containing 2 L of buffer I (20 mM sodium phosphate, 250 mM sucrose, 10 mM 2-mercaptoethanol, 2 mM Na_2EDTA, 1 mM dithiothreitol, 0.1 mM phenylmethanesulfonyl fluoride, 0.7 mg/L pepstatin, 0.5 mg/L leupeptin, and 10 μM each L-1-(tosylamino)-2-phenylethyl chloromethyl ketone and N^{α}-p-tosyl-L-lysine chloromethyl ketone, pH 7.4) and centrifuged for 20 min at 20000g. The supernatant fraction was decanted through glass wool, and solid ammonium sulfate was added over a 20-min period to 43% saturation (245 g/L) while the pH was maintained at 7.4. The mixture was stirred for 20 min and centrifuged for 20 min at 20000g, and the precipitate was discarded. The supernatant was adjusted to 75% saturation with solid ammonium sulfate (201 g/L) and centrifuged, and the pellet was resuspended in 180 mL of buffer II (5 mM sodium phosphate, 5 mM 2-mercaptoethanol, 0.5 mM dithiothreitol, and 0.5 mM Na_2EDTA, pH 7.4) and dialyzed overnight against two 14-L changes of buffer until the conductivity was less than 1.8 mΩ^{-1}.

Step 2: Chromatography on DEAE-Trisacryl. The dialyzed enzyme solution was clarified by centrifugation and applied, in series, to a Trisacryl GF-05 column (2.5 × 16 cm) and a DEAE-Trisacryl column (5 × 18 cm) equilibrated at 4 °C with buffer II. After washing with 1200 mL of buffer II, the enzyme was eluted with a 1200-mL linear gradient of 5–100 mM total concentration of sodium phosphate in buffer II. Fractions of peak activity were pooled, and the enzyme was concentrated by ammonium sulfate precipitation (85% saturation; 560 g/L) and resuspended as a clear solution in 30 mL of buffer III (20 mM sodium phosphate, 0.1 M KCl, 5 mM 2-mercaptoethanol, 0.5 mM dithiothreitol, and 0.5 mM Na_2EDTA, pH 7.4).

Step 3: Chromatography on Sephadex G-75. The concentrated enzyme sample was applied to a Sephadex G-75 column (2.5 × 100 cm) equilibrated at 4 °C with buffer III and eluted at 30 mL/h with buffer III. Fractions of peak activity were pooled.

Step 4: Chromatography on Red Agarose. The enzyme sample was applied to a reactive red 120 agarose column (1.5 × 30 cm) equilibrated at 4 °C with buffer III. After washing with 200 mL of buffer III, the enzyme was eluted with a 400-mL linear gradient of 0.1–0.8 M total concentration of KCl in buffer III. Fractions of peak activity were pooled and dialyzed against two changes of 20 volumes of buffer IV (1 mM sodium phosphate, 5 mM 2-mercaptoethanol, 0.5 mM dithiothreitol, and 0.5 mM Na_2EDTA, pH 7.4).

Step 5: Chromatography on Hydroxyapatite. The dialyzed enzyme sample was applied to a Bio-Gel HTP column (2.5 × 30 cm) equilibrated at 4 °C with buffer IV. After washing with 150 mL of buffer IV, the enzyme was eluted with a 600-mL linear gradient of 1–300 mM total concentration of sodium phosphate in buffer IV. The fractions of peak activity were pooled, concentrated by ultrafiltration (Amicon PM-10) to 2.5 mg/mL, dialyzed against 50 volumes of buffer III containing no KCl, and stored at 4 °C until use.

Results

Purification and Properties of the Enzyme. ALR2 was purified from bovine kidney by using a modification of the method of Daly and Mantle (1982), in which reactive red 120 agarose was substituted for Procion Orange MX-G as the dye–ligand chromatography matrix, and a final hydroxyapatite chromatography step was included. The enzyme was identified as ALR2 on the basis of chromatographic behavior, pI, substrate activity profile, and molecular mass. Data for the complete purification procedure, resulting in enzyme of >95%

Table I: Purification of Bovine Kidney Aldose Reductase

step	volume (mL)	protein (mg)	activity[a] (units)	specific activity (units/mg)	purification factor (-fold)	yield (%)	intrinsic specific activity[b] (units/mg)
homogenate[c]	1900	29500					
$(NH_4)_2SO_4$ (43–75%)	750	10300	16.6[d]	0.0016	1.0	100	0.18
DEAE-Trisacryl	110	1200	15.9	0.013	8.2	96	0.19
Sephadex G-75	65	100	10.8	0.11	67	65	0.29
red agarose	110	35	6.8	0.19	120	41	0.21
hydroxyapatite	110	31	6.4	0.21	130	38	0.20
activated enzyme	12	31	108.0	3.5	2190	650	3.5

[a] Activity measured at 25 °C as described under Experimental Procedures. Assay mixture contained 100 mM sodium phosphate buffer (pH 7.2), 5 mM DL-glyceraldehyde, 0.16 mM NADPH, 0.1 mM dithiothreitol, and 0.1 mM Na_2EDTA. [b] [Activity (units)]/[aldose reductase (mg)]; enzyme amount determined by quantitative Western blot procedure as described under Experimental Procedures. [c] From 900 g of bovine kidney medulla. [d] Assay contained inhibitor cocktail (1 mM each of barbitone, sodium valproate, and pyrazole) to inhibit other NADPH-dependent activities.

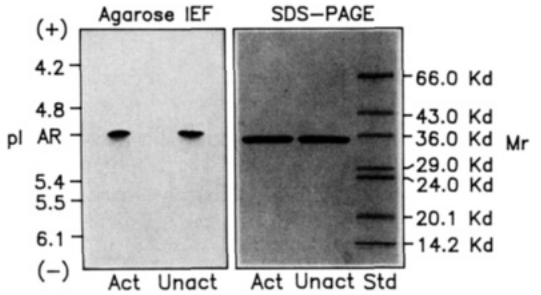

FIGURE 1: Comparative analysis of activated and unactivated ALR2 by agarose isoelectric focusing and SDS–PAGE. Activated and unactivated ALR2 (3.5 μg/lane) were focused in a 1 mm agarose slab gel containing 5 mM dithiothreitol and 2.0% (w/v) pH 4.5–5 and 0.5% (w/v) pH 3–10 ampholytes. Identical samples (1.2 μg/lane) were analyzed by SDS–PAGE in 11% polyacrylamide gels. Standard proteins were used to establish the indicated p*I* and relative M_r scale, and the protein bands were detected with silver stain as described under Experimental Procedures.

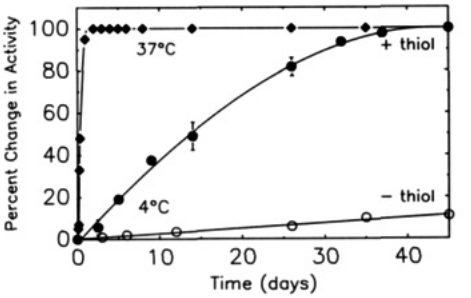

FIGURE 2: Temperature and thiol dependence of activation of purified ALR2. Activity was measured at 25 °C in an assay mixture containing 100 mM sodium phosphate buffer (pH 7.2), 160 μM NADPH, 5 mM DL-glyceraldehyde, 0.1 mM Na_2EDTA, and 0.1 mM dithiothreitol. Percent change in activity was calculated as $[(A_t - A_0)/(A_\infty - A_0)] \times 100$, where A_0, A_t, and A_∞ are the specific activity at time 0, t, and after complete activation, respectively. Results are shown for activation of enzyme stored at 4 °C in 20 mM sodium phosphate/0.5 mM Na_2EDTA buffer (pH 7.4) containing no thiols (○) or 5 mM 2-mercaptoethanol/0.5 mM dithiothreitol (●; average of four preparations). Activation at 37 °C in the same buffer containing thiols is also shown (◆).

purity, are summarized in Table I. At the final stage, the enzyme was almost completely homogeneous as judged by SDS–PAGE and agarose isoelectric focusing (Figure 1). The p*I* of 5.0 estimated by the latter technique was confirmed by chromatofocusing (data not shown). The strict maintenance of a reducing environment during the isoelectric focusing analysis eliminated the apparent microheterogeneity observed previously for purified samples of the enzyme (Grimshaw & Mathur, 1984). Enzyme activity eluted from Sephadex G-75 with an apparent M_r (35 000) identical with that seen by SDS–PAGE, and thus the enzyme is active as a monomer. We observed no evidence for an active dimer or higher M_r species. A stoichiometry of 1.0 mol of $NADP^+$/mol of enzyme ($K_d \leq$ 50 nM) was determined by fluorescence titration. Purified enzyme contained no carbohydrate moieties as assayed by the thymol–sulfuric acid method (Gander, 1984).

Activation of the Purified Enzyme. The specific activity of the purified enzyme increased during storage at 4 °C from 0.2 unit/mg to a maximum of 3.5 units/mg (DL-glyceraldehyde; standard assay) (Figure 2). The half-time for activation at 4 °C was 14 days. At 37 °C, the rate of activation was variable, with a minimum half-time of 5 h. An activation energy of 21 kcal/mol was calculated from the temperature variation of the rate. Activation was faster when thiols were present (Figure 2) (dithiothreitol and 2-mercaptoethanol were equally effective), but was not affected by ionic strength [0.4 M NaCl or $(NH_4)_2SO_4$] or buffer type (phosphate versus Mops) (data not shown). No change in relative M_r, p*I*, or homogeneity of the enzyme was detected by SDS–PAGE or agarose isoelectric focusing (Figure 1) following activation, indicating that the effect was not due to proteolysis or deamidation. Activation of the purified enzyme was often accompanied by the formation of a flocculent protein precipitate. In addition, partially purified enzyme samples obtained during the purification process also underwent activation. For example, a sample from the ammonium sulfate fractionation step increased 2.5-fold in activity over 5 days at 4 °C.

Determination of the Intrinsic Specific Activity. After each step of the purification procedure, the intrinsic specific activity was calculated as the ratio of enzyme activity, measured by using the standard assay, to the amount of ALR2 protein, estimated by the quantitative Western blot procedure. As shown in the last column of Table I, the intrinsic specific activity remained constant at 0.21 ± 0.04 unit/mg during the purification procedure. As a control, standard curves were constructed by using purified samples of the activated and unactivated enzyme, and the immunoradiographic response for quantitation by Western blot was shown to be the same. Accurate activity assays were not possible at the homogenate stage because of interference by other NADPH-utilizing activities.

Protein Fluorescence. Fluorescence spectra (uncorrected) for the two enzyme forms had similar features [λ_{max} (excitation) = 285 nm; λ_{max} (emission) = 340 nm], but the activated enzyme showed a 30% enhancement of fluorescence relative to the unactivated form (data not shown). Formation of the binary E–$NADP^+$ complex resulted in 72% and 58% quenching of the protein fluorescence with the unactivated and activated enzyme, respectively.

Circular Dichroism. Figure 3 shows the average of circular dichroism spectra measured in triplicate for two preparations

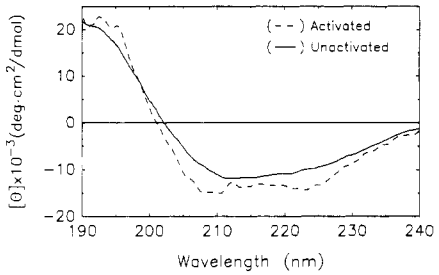

FIGURE 3: Comparison of circular dichroism spectra for the activated and unactivated enzyme. Circular dichroism spectra of the enzyme (1.54 μM active sites in 20 mM sodium phosphate/0.1 mM Na_2EDTA buffer, pH 7.2) were recorded at 25 °C under constant nitrogen flush by using a 0.10 cm path length quartz cell. The spectra shown were averaged over triplicate measurements of two preparations each of activated (---) and unactivated (—) enzyme. Multiple linear regression analysis of the spectra, as described under Experimental Procedures, gave the following secondary structure composition (mean ± SE) for the activated (38 ± 3% α-helix, 22 ± 4% β-sheet, 10 ± 3% β-turn, and 30 ± 3% random coil) and unactivated (49 ± 4% α-helix, 6 ± 8% β-sheet, 14 ± 5% β-turn, and 31 ± 6% random coil) enzyme forms.

of the activated and unactivated enzyme. Analysis of the spectral data by the AVIV multiple linear regression program gave the following secondary structure composition (mean ±SE) for the unactivated (49 ± 4% α-helix, 6 ± 8% β-sheet, 14 ± 5% β-turn, and 31 ± 6% random coil) and activated (38 ±3% α-helix, 22 ± 4% β-sheet, 10 ± 3% β-turn, and 30 ± 3% random coil) enzyme forms. The correlation coefficients (r) obtained from the multiple linear regression analyses were in all cases ≥0.993.

Chemical Modification of Cysteine Sulfhydryls. Reaction with DTNB indicated that all cysteine sulfhydryls were reduced and were accessible under nondenaturing conditions for the unactivated (5.9 ± 0.3 mol of SH/mol) and activated (5.8 ± 0.3 mol of SH/mol) enzyme, respectively. Reaction of the first thiol group of either enzyme form was complete within 10 s. The second-order rate constants for reaction of DTNB with the remaining cysteines were 33 and 66 M^{-1} min^{-1} for the unactivated and activated enzyme, respectively. Unactivated enzyme showed a steady decrease in catalytic activity during the course of the DTNB reaction, with 60%, 40%, and 25% activity remaining after 1, 2, and 3 mol of SH/mol of enzyme had reacted, respectively. Conversely, activated enzyme showed an initial increase in activity, with 130%, 100%, and 60% activity remaining after 1, 2, and 3 mol of SH/mol of enzyme had reacted, respectively.

Determination of Kinetic Parameters. Double-reciprocal plots of $1/v_i$ versus 1/[aldehyde] determined with the unactivated enzyme displayed two, and sometimes three, distinct regions, which were (in order of increasing aldehyde concentration) (1) a linear asymptote region (1/[aldehyde] → ∞), (2) a region of downward curvature (apparent substrate activation), and (3) a region of upward curvature (substrate inhibition). Representative plots for glycolaldehyde, D-glucose, and p-nitrobenzaldehyde are shown in Figure 4. V and V/K_b (B = aldehyde) values for the unactivated enzyme were determined by least-squares analysis of the data obtained by using freshly purified enzyme. The data were fit to eq 3 when the plot was linear and to eq 4 when substrate inhibition was observed, and data from the asymptote and substrate activation regions (regions 1 and 2) were fit to eq 5 when all three regions were apparent. The plot shown for glycolaldehyde with the unactivated enzyme (see inset, Figure 4A) is an example of the latter case. [The rate contribution in region 2 was due to a small amount (≤1.5%) of the activated form.] Data for the activated enzyme were fit to eq 3 if the plot was linear or

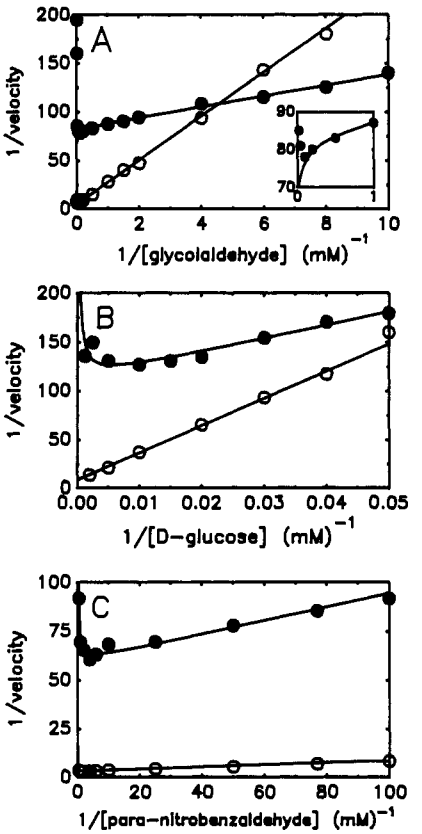

FIGURE 4: Double-reciprocal plots for aldehyde substrates with activated and unactivated ALR2. Initial velocity data shown for glycolaldehyde (A), D-glucose (B), and p-nitrobenzaldehyde (C) were determined by using activated (○) and unactivated (●) ALR2 as described under Experimental Procedures. Assays were conducted at 25 °C in 50 mM MOPSED buffer (pH 7.0) containing 160 μM NADPH and the indicated concentration of aldehyde substrate. The inset is an expansion of the region for [glycolaldehyde] ≥ 1 mM using the unactivated enzyme; the downward curvature is due to a small amount (≤1.5%) of the activated enzyme form. The points represent the experimental values, and the curves are calculated from fits to eq 3, 4, or 5.

to eq 4 if substrate inhibition was observed. A comparison of the kinetic parameters determined for a series of aldehyde substrates with the unactivated and activated enzyme (Table II) shows that while the turnover number (V/E_t) for each enzyme form varied less than 3-fold over this series of aldehyde substrates, V/K_b varied 7600-fold for the unactivated and 47 500-fold for the activated enzyme forms, respectively. V/E_t increased an average of (17 ± 4)-fold upon activation of the enzyme, while V/K_b either increased or decreased up to 4-fold, depending on the substrate. Table II also lists the kinetic parameters for NADPH, determined from fits to eq 7 of the initial velocity data obtained with glycolaldehyde as the substrate. The apparent dissociation constant for NADPH (K_{ia}) determined from the same analysis decreased from 1.0 ± 0.1 μM for the unactivated to ≤0.2 μM for the activated enzyme. These values are at least 20- and 4-fold larger than the maximum K_d value (≤50 nM) for the E·NADPH binary complex, estimated by fluorescence titration. Substrate inhibition by glycolaldehyde was partial uncompetitive versus NADPH (data not shown), with $V_{inhibited}$ equal to 30% and 5% of V for the unactivated and activated enzyme, respectively.

Inhibitors and Activators. K_i values determined for simple inhibition (Dixon, 1953) by AL-1576 and Statil (activated enzyme only), Epalrestat, and Sorbinil and for reversible tight-binding inhibition [i.e., inhibition where $K_i \approx [E_t]$ (Williams & Morrison, 1979)] by AL-1576 and Statil (unactivated enzyme only) and Tolrestat (both enzyme forms)

Table II: Comparison of Kinetic Parameters for Activated and Unactivated Enzyme[a]

substrate	activated[b] V/E_t (min^{-1})	activated[b] V/KE_t (mM^{-1} min^{-1})	unactivated[c] V/E_t (min^{-1})	unactivated[c] V/KE_t (mM^{-1} min^{-1})	ratio (activated/unactivated) V/E_t	ratio (activated/unactivated) V/KE_t
glycolaldehyde	71 ± 2	14 ± 2	4.1 ± 0.1	60 ± 5	17	0.24
D-glyceraldehyde	124 ± 4	730 ± 60	4.7 ± 0.1	390 ± 60	26	1.9
L-glyceraldehyde	72 ± 2	25 ± 2	4.9 ± 0.1	19 ± 1	15	1.3
D-xylose	77 ± 3	1.1 ± 0.1	4.6 ± 0.1	4.6 ± 0.3	17	0.23
D-glucose	41 ± 2	0.12 ± 0.01	3.2 ± 0.1	0.25 ± 0.02	13	0.48
p-chlorobenzaldehyde	71 ± 2	1100 ± 50	4.7 ± 0.1	850 ± 80	15	1.3
p-nitrobenzaldehyde	108 ± 9	5700 ± 400	5.9 ± 0.2	1500 ± 200	18	3.8
pyridine-3-carboxaldehyde	107 ± 2	4300 ± 500	6.4 ± 0.2	1900 ± 100	17	2.3
indole-3-acetaldehyde	61 ± 3	600 ± 100	4.0 ± 0.2	660 ± 180	15	0.91
NADPH[d]	71 ± 2	71000 ± 16000	4.1 ± 0.1	4600 ± 1200	17	15

[a] Assays conducted at 25 °C in 50 mM MOPSED buffer (pH 7.0) containing 0.16 mM NADPH. [b] Values obtained from fits to eq 3 or 4. [c] Values obtained from fits to eq 5 correspond to the asymptote region of the curves ($1/[A] \rightarrow \infty$); otherwise, values obtained from fits to eq 3 or 4. [d] Values obtained from fits to eq 7; glycolaldehyde was used as the aldehyde substrate.

Table III: Comparison of Aldose Reductase Inhibitor Potency with Activated and Unactivated Enzyme[a]

aldose reductase inhibitor	$K_{i,act}$ (μM)	$K_{i,unact}$ (μM)	ratio ($K_{i,act}/K_{i,unact}$)	stoichiometry (mol of I/mol of E)
Tolrestat (AY-27773)	0.050 ± 0.005[b]	0.021 ± 0.002[b]	2.5	3.0 ± 0.5
Statil (ICI-128436)	35 ± 5	0.20 ± 0.03[b]	170	0.9 ± 0.1
AL-1576	50 ± 5	0.25 ± 0.09[b]	200	1.0 ± 0.1
Epalrestat (ONO-2235)	4.0 ± 0.2	2.0 ± 0.2	2.0	
Sorbinil (CP-45634)	200 ± 10	30 ± 4	6.6	

[a] For simple inhibition (Dixon, 1953), the velocity was measured at 25 °C in 50 mM MOPSED buffer (pH 7.0) containing 10 mM glycolaldehyde and 0.16 mM NADPH. $K_{i,act}$ and $K_{i,unact}$ are the apparent K_i values determined from fits to eq 9 of data obtained with activated and unactivated enzyme, respectively. [b] For reversible tight-binding inhibition (Williams & Morrison, 1979), the velocity was measured as described in footnote *a* or by using a fluorometric assay method with 20 μM NADPH. Apparent K_i values were obtained from fits to eq 11.

are listed in Table III. Activation reduced the potency of the five ALR2 inhibitors; the apparent K_i value increased from 2-fold for Epalrestat to 200-fold for AL-1576. A representative plot of data for tight-binding inhibition of unactivated enzyme by Statil is shown in Figure 5; similar results were obtained with AL-1576 and Tolrestat. The stoichiometries of tight-binding inhibition determined from fits to eq 11 were (expressed as moles of inhibitor per mole of enzyme active site) 0.9 ± 0.1 for Statil, 1.0 ± 0.1 for AL-1576, and 3.0 ± 0.5 for Tolrestat. The stoichiometry for Tolrestat was not affected by the activation state of the enzyme. The apparent K_i values shown in Table III were not altered by changes in the concentration of aldehyde (0.1 or 10 mM glycolaldehyde) or nucleotide (10 or 160 μM NADPH), indicating that the site of inhibition is distinct from the catalytic site.

When sulfate (Na^+ or NH_4^+) was tested as an effector with glycolaldehyde as the variable substrate ([NADPH] = 20 μM), the result was hyperbolic slope activation ($K_{act,s}$ = 28 mM) and linear intercept inhibition (K_{ii} = 540 mM) with the unactivated enzyme, but only linear noncompetitive inhibition ($K_{is} = K_{ii} \approx 1.3$ M), and no activation, with the activated enzyme (data not shown). The reaction was no longer stimulated by sulfate once activation had occurred, and only the inhibitory component remained.

Estimation of the Amount of Enzyme in the Activated State. The extent of activation was estimated by two independent methods. The first method, based on the difference in kinetic parameters for the two activation states (Table II), involved deconvolution of data from a biphasic double-reciprocal plot (not including the region of substrate inhibition) into the two activity components of eq 6 (V_1 and V_2), as described above. The fraction of enzyme in the two activation states, E_{act}/E_t and E_{unact}/E_t, was then calculated from

$$(V_2/V_1)_{obsd} = (V_{act}/V_{unact})([E_{act}]/[E_{unact}]) \quad (12)$$

$$([E_{act}]/[E_t]) = \{1 + [(V_{act}/V_{unact})(V_1/V_2)]\}^{-1} \quad (13)$$

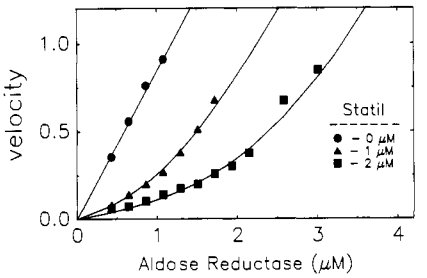

FIGURE 5: Tight-binding inhibition of unactivated enzyme by Statil. Initial velocity was measured at 25 °C in 50 mM MOPSED buffer (pH 7.0) containing 10 mM glycolaldehyde and 160 μM NADPH. The points are the experimental values, and the curve is calculated from a fit to eq 11 with K_i = 0.20 μM, V = 0.84 μM^{-1}, and p = 0.9 ± 0.1 (number of binding sites). The data were corrected for a small (10%) velocity contribution from the less sensitive activated enzyme form.

Equation 12 states that the ratio of the observed maximum velocities, $(V_2/V_1)_{obsd}$, is equal to the ratio of the true maximum velocities, (V_{act}/V_{unact}) = 17 (e.g., glycolaldehyde), multiplied by the ratio of the two enzyme forms. Solving for $[E_{unact}]$ in eq 12 and substituting into the expression $[E_t] = [E_{act}] + [E_{unact}]$, one obtains eq 13, which gives the fraction of enzyme in the activated state as a function of known quantities. The second method, which was based on the difference in K_i values for inhibition by AL-1576 or Statil (Table III) and involved deconvolution of data from a biphasic Dixon plot according to eq 10, gave similar results when initial velocities were measured at concentrations of the two substrates that were saturating for both enzyme forms (data not shown). However, due to the 17-fold difference in V_{act} and V_{unact}, these methods cannot detect a small amount of the unactivated form in a highly active enzyme sample. For this purpose, inhibition by AL-1576 or Statil was measured at 0.1 mM glycoaldehyde, which is comparable to $K_{b,unact}$ = 0.07 mM, but a factor of 50 lower than $K_{b,act}$ = 5 mM. At this

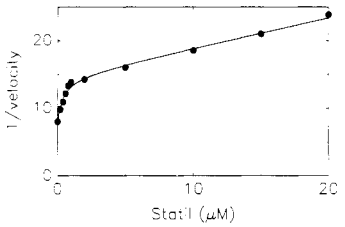

FIGURE 6: Biphasic Dixon plot for inhibition of partially activated enzyme by Statil. Initial velocity was measured at 25 °C in 50 mM MOPSED buffer (pH 7.0) containing 0.1 mM glycolaldehyde and 20 μM NADPH. The points are the experimental values, and the curve is calculated from a fit to eq 5, which is a rearrangement of eq 10, with K_{i1} = 33 μM, K_{i2} = 0.21 μM, V_1 = 0.075, and V_2 = 0.060. Since the apparent (V_{act}/V_{unact}) = 0.57 at 0.1 mM glycolaldehyde, a calculation using eq 12 and 13 shows that E_{act} = 69% and E_{unact} = 31% of the total enzyme.

aldehyde concentration, the ratio of apparent velocities, $(V_{act}/V_{unact})_{obsd}$, is reduced from 17 to 0.57, and the unactivated velocity component (V_{unact}) for a sample containing 30% E_{unact} is increased from 2.5% to 43% of $V_{total} = V_{act} + V_{unact}$. Figure 6 shows the results obtained for Statil inhibition at 0.1 mM glycolaldehyde for an enzyme sample containing 31% E_{unact} and 69% E_{act}.

Discussion

During storage at 4 °C, the specific activity of purified bovine kidney ALR2 increased from 0.2 to 3.5 units/mg (Figure 2). The most pronounced effect of the activation process was on the reaction kinetics, as indicated by the change in the double-reciprocal plot for the aldehyde substrate (Figure 4). Ignoring substrate inhibition, the change from a concave down plot with a low-V_{max} asymptote (see inset, Figure 4A) to a linear plot with a high V_{max} suggested that there were two catalysts present in the reaction mixture during activation, with the proportion of the high-velocity component increasing from almost zero to become the predominant species. Analysis of the kinetic data using a two-enzyme model (eq 6) showed that the sum of two components quantitatively accounted for the nonlinear double-reciprocal plots observed over the entire time course of enzyme activation.

The kinetic data were consistent with the presence of two enzymes that catalyze the same reaction with different kinetic parameters. Analysis by SDS–PAGE and isoelectric focusing, however, showed that the enzyme preparation consisted of a single, homogeneous protein which did not change in apparent M_r, pI, or homogeneity during the course of activation (Figure 1). The two catalysts must thus be different forms of the same enzyme, ALR2. In support of this conclusion, several experiments indicated that significant changes in the secondary structure had occurred during activation, including (1) an increase in the intrinsic protein fluorescence, (2) a decrease in the amount of fluorescence quenching upon formation of the binary E·NADP$^+$ complex, (3) an increase in the rate of reaction of the enzyme's cysteine sulfhydryl groups with DTNB, and (4) a reversal of the effect of thiol modification on the catalytic rate, from inhibition to activation.

Perhaps the best evidence for a conformational change has come from comparison of the circular dichroism spectra of the two enzyme forms (Figure 3), which indicated that the secondary structure had changed from one comprised of 49 ± 4% (mean ± SE) α-helix and 6 ± 8% β-sheet to one that consisted of 38 ± 3% α-helix and 22 ± 4% β-sheet. (The percentages of β-turn and random coil were not significantly different for the two enzyme forms.) Changes in the circular dichroism spectrum, similar in magnitude to those reported here, also occur when the inhibitory peptide, Kemptide, binds to cAMP-dependent protein kinase (Reed & Kinzel, 1984). To our knowledge, however, this is the first example of such a conformational change for an unliganded enzyme. Further insight into the structural basis for activation must await the X-ray crystallographic determination of the three-dimensional structure, the preliminary results of which have recently been reported (Winkler et al., 1987; Rondeau et al., 1987).

Scheme I: Proposed Reaction Mechanism for ALR2[a]

$$E \underset{k_2}{\overset{k_1A}{\rightleftharpoons}} EA \underset{k_4}{\overset{k_3B}{\rightleftharpoons}} (EAB \rightleftharpoons E^*PQ) \underset{k_6P}{\overset{k_5}{\rightleftharpoons}} E^*Q \underset{k_8Q}{\overset{k_7}{\rightleftharpoons}} E^* \underset{k_{10}}{\overset{k_9}{\rightleftharpoons}} E$$

[a] A = NADPH; B = glycolaldehyde; P = ethylene glycol; Q = NADP$^+$.

The alternative explanations for the biphasic kinetic behavior are not consistent with our experimental results. Substrate activation, similar to that described for alcohol dehydrogenase (Dalziel & Dickinson, 1966), has been proposed for rat lens ALR2 (Doughty & Conrad, 1982) on the basis of earlier studies of the enzyme isolated from *Rhodotorula* (Sheys & Doughty, 1971). In this mechanism, apparent substrate activation occurs because the product, NADP$^+$, is released at a faster rate from the ternary E·NADP$^+$·aldehyde complex, which is formed at high aldehyde concentrations, than it is released from the binary E·NADP$^+$ complex in the final step of the normal reaction mechanism. However, our data indicated that formation of the dead-end E·NADP$^+$·aldehyde complex with ALR2 resulted in substrate inhibition (uncompetitive versus NADPH) and not substrate activation.

p-Chlorobenzaldehyde, which is not hydrated to any significant extent in aqueous solution at neutral pH (Sander & Jencks, 1968), displayed nonlinear kinetic behavior analogous to that of the other aldehydes tested. The addition of thiols to the assay mixture also had little effect on the kinetic patterns. Thus, significant activity of the hydrate or thiohemiacetal form of the substrate also cannot account for the biphasic kinetic plots.

On the basis of an analysis of the changes in the individual kinetic parameters that occurred as a result of activation, we propose a mechanism for the ALR2 reaction that includes an isomerization of the free enzyme as the step primarily affected by the activation process (Scheme I).[2] In this mechanism, the apparent kinetic dissociation constant for NADPH, $K_{ia} = (k_2/k_1)(1 + k_{10}/k_9)$, is equal to the true dissociation constant, $K_d = k_2/k_1$, multiplied by the factor $(1 + k_{10}/k_9)$. The K_d value determined by fluorescence titration can thus be lower than K_{ia} if the isomerization equilibrium favors E* (K_{iso} = [E]/[E*] = $k_9/k_{10} < 1$).[3] The kinetic expression for V/K_a, which for an ordered mechanism is equal to k_1, becomes $k_1/(1 + k_{10}/k_9)$ when the isomerization step is included. The expression for $V = 1/(1/k_5 + 1/k_7 + 1/k_9)$ also includes a term

[2] If the uncompetitive (versus NADPH) substrate inhibition by glycolaldehyde is partial, rather than total, because of a slow release of NADP$^+$ from the E·NADP$^+$·aldehyde dead-end complex, then the reaction may show some degree of randomness if NADPH can then bind to E·aldehyde to form a productive complex. The small contribution of this alternative pathway at high aldehyde concentrations will not, however, affect the conclusions of the kinetic analysis.

[3] The fluorescence binding data require either that NADPH bind to E* or that equilibration of E and E* be rapid. A calculation of the half-time for conversion of E* to E ($t_{1/2}$ = 10 and ≤1 s for the unactivated and activated enzyme, respectively), based on the values determined for k_9, indicates that equilibration is rapid. However, should NADPH bind to E*, this complex cannot then bind B and proceed to catalysis, since the kinetic predictions for an isomerization of E·A do not agree with the experimental results.

for this step, but isomerization of the free enzyme has no effect on $V/K_b = k_3k_5/(k_4 + k_5)$.

As shown in Table II, the turnover numbers (V/E_t) determined for a series of aldehyde substrates, which included short- and long-chain aldoses and aromatic aldehydes, all increased an average of 17-fold upon activation of the enzyme. Analysis of the initial velocity patterns for NADPH and glycolaldehyde showed that V/K_a also increased 15.4-fold and K_{ia} decreased at least 5-fold. The changes in V/K_b, which ranged from a 4-fold decrease for glycolaldehyde to a 4-fold increase for *p*-nitrobenzaldehyde, did not correlate with the increase in V/E_t. In addition, recall that the dissociation constants for NADPH binding obtained by fluorescence titration ($K_d \leq 50$ nM) were at least 4-fold and 20-fold lower than the K_{ia} value obtained from the kinetic data for the activated and unactivated enzyme, respectively. Comparison of the kinetic expressions for each of the parameters consistently affected by activation, namely, V, V/K_a, and K_{ia}, but not V/K_b, reveals that k_9 is the only common factor. Thus, if we assume that k_9 is the rate constant primarily affected by activation, then we can use this information to calculate values for each of the rate constants for the first and last steps in Scheme I (k_1, k_2, k_9, and k_{10}), using glycolaldehyde as the example.

To explain the increase in V after activation, k_9 must be rate determining for the unactivated enzyme reaction ($k_9 = 4.1$ $min^{-1} = V_{unact}$) and increase by at least a factor of 17 in the activated reaction ($k_9 \geq 71$ $min^{-1} = V_{act}$). If we assume the minimum value, $k_9 = 71$ min^{-1}, then we can calculate that $k_{10} = 500$ min^{-1} from the experimental ratio $(V/K_a)_{act}/(V/K_a)_{unact} = 15.4$, since the k_1 terms in the kinetic expression for this ratio cancel (activation does not affect k_1) and the k_9 values have already been assigned. A comparison of the calculated values for the factor $(1 + k_{10}/k_9)$, which are 8 and 120 for activated and unactivated enzyme, respectively, with the estimates of 4 and 20 determined by dividing the kinetic K_{ia} value by the upper limit for K_d, indicates that the true K_d may be in the 5–10 nM range. From the expression for V/K_a and the experimental value for this parameter (Table II), we can calculate a value for k_1, the on-rate for NADPH, of 5×10^8 M^{-1} min^{-1}. The expression $k_2 = K_dk_1$ yields a value for k_2, the off-rate for NADPH, of ≤ 25 min^{-1}, which is intermediate between the values for V_{act} and V_{unact} for the forward reaction.[4]

The foregoing analysis indicates that the forward reaction is limited, at least for the unactivated enzyme, by the forward rate of isomerization (k_9). If k_9 increases more than 17-fold, this step will no longer be rate limiting for the activated enzyme, and k_{10} will increase accordingly, with the minimum value for k_{10}/k_9 set by the experimental ratio $[(K_{ia}/K_d) - 1]$. However, the ratio $(k_{10}/k_9)_{unact}/(k_{10}/k_9)_{act}$, which is equal to the ratio of the equilibrium contants for the isomerization step ($K_{iso,act}/K_{iso,unact}$), is constrained by the increase in V/K_a and must have a value in the range 15–17. The primary effect of activation, therefore, is a 15–17-fold increase in K_{iso}. Sulfate may also exert its effect at the isomerization step, since sulfate no longer shows stimulation of the reaction after activation of the enzyme has occurred, but simply displays the inhibitory effect due to competition at the NADPH binding site of either enzyme form. In the reverse reaction, k_2 may be the slow step, since the reverse reaction of the rat lens enzyme proceeds at a rate that is at least 6-fold slower than the rate of the forward reaction (Griffin & McNatt, 1986).

[4] The value for $k_2 = k_1K_d$ is insensitive to the value chosen for k_{10}/k_9 since the change in $k_1 = (V/K_a)[1 + (k_{10}/k_9)]$ will offset the change in $K_d = K_{ia}/[1 + (k_{10}/k_9)]$.

The relative potency of the five compounds tested as inhibitors of bovine kidney ALR2 (Table III) is similar to that reported for preparations of the enzyme from other tissues and species (Dvornik, 1987b). Also in agreement with previous studies (Kador & Sharpless, 1983; Humber, 1987), inhibition apparently occurs at a site that is distinct from the catalytically active site, since changes in substrate concentration did not affect the K_i values. However, the change in binding affinity observed upon activation of the enzyme has not previously been recognized. For Statil and AL-1576, the increase in K_i value was substantial (about 200-fold), while for the remaining three compounds, including the most potent (Tolrestat) and least potent (Sorbinil) inhibitors, the increase was much less.

The large difference in K_i value for inhibition by AL-1576 and Statil has also provided a convenient method for estimation of the extent of enzyme activation, based on an analysis of the biphasic Dixon plots obtained with these inhibitors (Figure 6). More importantly, the change in the extent of enzyme activation estimated by this method exactly paralleled the change determined by analysis of the initial velocity data, consistent with the proposed two-state model for activation of the enzyme.

Analysis of the tight-binding inhibition data for the unactivated enzyme indicated a difference in binding stoichiometry; AL-1576 and Statil inhibited at a 1:1 molar ratio, while inhibition by Tolrestat required a 3:1 ratio. The difference in ARI binding stoichiometry and in the sensitivity of K_i to changes in the activation state suggests that the ARIs bind at more than one site on the enzyme. The five compounds tested as inhibitors are structurally quite diverse, however, and more work will be required to establish which structural features are important for binding and sensitivity to activation.

The potential therapeutic application of an effective ARI for the prevention and treatment of diabetic complications has generated a great deal of interest in understanding the mode of action of these compounds, and several attempts have been made to model the ARI binding site on the basis of structure–activity correlations (Kador & Sharpless, 1983; Brittain et al., 1987). Interspecies differences in ARI K_i values have been attributed to small differences in the primary structure of the enzyme (Flynn, 1982b). However, changes in the extent of enzyme activation could also account for the reported differences, since activation has a pronounced effect on the ARI K_is (Table III). The effect of activation would thus be to mask an underlying similarity among the various mammalian ALR2 gene products, which has been shown by chemical, physical, and kinetic methods (Conrad & Doughty, 1982), by demonstration of interspecies cross-immunoreactivity (Mathur & Grimshaw, 1986; Morjana & Flynn, 1989), and by comparison of the primary amino acid sequences (Carper et al., 1987; Doughty et al., 1988; Morjana et al., 1989).

The intrinsic specific activity of the enzyme remained essentially constant throughout the purification procedure (Table I), although activation would occur slowly in samples removed as early as the ammonium sulfate fractionation step. Activation, therefore, does not appear to result from reactivation of enzyme that has been inactivated during isolation. Since activation is a thermodynamically favorable process, which eventually leads to the fully activated enzyme, there must be a mechanism for maintaining the unactivated state in vivo. One possibility is suggested by the report of a heat-stable, dissociable factor that can alter the catalytic activity and sensitivity to inhibition of human placental ALR2 (Maragoudakis et al., 1984). The ability of high salt to activate the bovine lens enzyme has been shown to fluctuate, depending

on the season in which the animals are slaughtered (Del Corso et al., 1987). Regardless of the detailed mechanism, activation provides a novel means for regulation of this enzyme in vivo, which may be important in the modulation of ALR2 activity shown to occur in diabetes (Akagi et al., 1987).

Kinetic data consistent with activation have also been described for ALR2 isolated from other mammalian species. A similar activation process occurs for an NADPH-dependent aldo–keto reductase isolated from human erythrocytes (Srivastava et al., 1985). Furthermore, a survey of the ALR2 literature reveals that the K_b and relative V_{max} values determined with the bovine kidney enzyme, in particular for glyceraldehyde, glucose, and xylose, are similar to those values reported for enzyme preparations from a number of different species, all of which show biphasic double-reciprocal plots (Hastein & Velle, 1969; Sheaff & Doughty, 1976; Hoffman et al., 1980; Daly & Mantle, 1982; Halder & Crabbe, 1984; Poulsom, 1986). For those preparations that show linear double-reciprocal plots (Boghosian & McGuinness, 1979; Branlant, 1982; Wermuth et al., 1982; Cromlish & Flynn, 1983a,b; Hara et al., 1983; Morjana & Flynn, 1989), either the reported specific activity indicates a fully activated enzyme or the reported K_b values are intermediate between those of the activated and unactivated forms. Computer simulation indicates that, for enzyme samples containing more than 20% activated form, the curvature of the double-reciprocal plot is quite gradual (data not shown), and a wide range of aldehyde substrate concentration is required to determine the curvature with any precision. Whether or not activation proves to be a general property of the mammalian enzyme remains to be established.

Activation also has consequences for the practical design of kinetic studies of ALR2, which can be seen by comparison of the double-reciprocal plots for D-glucose (Figure 4B) and *p*-nitrobenzaldehyde (Figure 4C). To illustrate the point, if we use 100 mM D-glucose and 0.5 mM *p*-nitrobenzaldehyde (pNBzCHO) as the standard assay concentrations, the ratio of observed velocities ($V_{pNBzCHO}/V_{glucose}$) will vary from 2 to 11, depending on the activation state of the enzyme. If activation occurs during purification of the enzyme, $V_{glucose}$ will appear to decrease relative to $V_{pNBzCHO}$, when, in fact, the V_{max} for both substrates is increasing at exactly the same rate. By the same reasoning, the apparent K_i value determined with each substrate will vary with the activation state of the enzyme, since the unactivated form is more susceptible to inhibition (cf. Table III). For example, given an enzyme sample composed of 50% E_{unact} and 50% E_{act}, and an inhibitor concentration sufficient to inhibit all the E_{unact} and none of the E_{act} (e.g., 5 μM AL-1576), the apparent percent inhibition will be 24% for D-glucose ($V_{unact}/V_{total} \approx 0.24$; $V_{act}/V_{total} \approx 0.76$) but only 5% for *p*-nitrobenzaldehyde ($V_{unact}/V_{total} \approx 0.05$; $V_{act}/V_{total} \approx 0.95$). Activation can thus account for the substrate-dependent change in inhibition that has been reported for ALR2 isolated from human retina (Poulsom, 1987) and pig brain (Cromlish & Flynn, 1985).

In summary, we have described a novel activation process for homogeneous bovine kidney ALR2 that results in marked changes in the secondary structure, kinetic properties, and sensitivity to inhibition of the enzyme. A detailed analysis of the kinetic parameters has lead to a proposed kinetic mechanism that includes a slow isomerization of the free enzyme as the step primarily affected by activation. Hopefully, the methods demonstrated for detecting the presence of the activated and unactivated enzyme forms, based on both initial velocity and inhibition studies, will encourage further work to determine the generality of the activation process in vitro and what role, if any, this process may have in the regulation of the enzyme in vivo.

ACKNOWLEDGMENTS

We thank Dr. F. M. Huennekens, Dr. T. G. Flynn, and Dr. C. C. Doughty for many helpful discussions and Linda L. Tennant for assistance with the circular dichroism measurements.

REFERENCES

Akagi, Y., Kador, P. F., & Kinoshita, J. H. (1987) *Invest. Ophthamol. Visual Sci. 28*, 163–167.

Blanchard, J. S., & Cleland, W. W. (1980) *Biochemistry 19*, 3543–3550.

Boghosian, R. A., & McGuinness, E. T. (1979) *Biochim. Biophys. Acta 567*, 278–286.

Bradford, M. M. (1976) *Anal. Biochem. 72*, 248–254.

Branlant, G. (1982) *Eur. J. Biochem. 129*, 99–104.

Brittain, D., Howe, R., Morris, J., & Wilkinson, A. (1987) *International Workshop on Aldose Reductase Inhibitors*, Dec 7–10, 1987, Honolulu, HI, Abstract P3, ICI Pharmaceuticals Group, Cheshire, U.K.

Carper, D., Nishimura, C., Shinohara, T., Dietzchold, B., Wistow, G., Craft, C., Kador, P. F., & Kinoshita, J. H. (1987) *FEBS Lett. 20*, 209–213.

Cassim, J. Y., & Yang, J. T. (1969) *Biochemistry 8*, 1947–1951.

Chang, C. T., Wu, C.-S. C., & Yang, J. T. (1978) *Anal. Biochem. 91*, 13–31.

Cleland, W. W. (1963) *Biochim. Biophys. Acta 67*, 104–137.

Cleland, W. W. (1979) *Methods Enzymol. 63*, 103–138.

Conrad, S. M., & Doughty, C. C. (1982) *Biochim. Biophys. Acta 708*, 348–357.

Cromlish, J. A., & Flynn, T. G. (1983a) *J. Biol. Chem. 258*, 3416–3424.

Cromlish, J. A., & Flynn, T. G. (1983b) *J. Biol. Chem. 258*, 3583–3586.

Cromlish, J. A., & Flynn, T. G. (1985) *J. Neurochem. 44*, 1485–1493.

Cromlish, J. A., Yoshimoto, C. K., & Flynn, T. G. (1985) *J. Neurochem. 44*, 1477–1484.

Daly, A. K., & Mantle, T. J. (1982) *Biochem. J. 205*, 373–380.

Dalziel, K., & Dickinson, F. M. (1966) *Biochem. J. 100*, 491–500.

Del Corso, A., Camici, M., & Mura, U. (1987) *Biochem. Biophys. Res. Commun. 148*, 369–375.

Dixon, M. (1953) *Biochem. J. 55*, 170–171.

Doughty, C. C., & Conrad, S. M. (1982) *Biochim. Biophys. Acta 708*, 358–364.

Doughty, C. C., Early, S. L., Schade, S. Z., & Williams, T. R. (1988) *FASEB J. 2*, A1746.

Dvornik, D. (1987a) in *Aldose Reductase Inhibition* (Porte, D., Ed.) pp 69–152, McGraw-Hill, New York.

Dvornik, D. (1987b) in *Aldose Reductase Inhibition* (Porte, D., Ed.) pp 221–323, McGraw-Hill, New York.

Flynn, T. G. (1982a) *Biochem. Pharmacol. 31*, 2705–2712.

Flynn, T. G. (1982b) *Prog. Clin. Biol. Res. 114*, 169–182.

Gabbay, K. H., & Cathcart, E. S. (1974) *Diabetes 23*, 460–468.

Gander, J. E. (1984) *Methods Enzymol. 104*, 447–448.

Griffin, B. W., & McNatt, L. G. (1986) *Arch. Biochem. Biophys. 246*, 75–81.

Griffin, B. W., McNatt, L. G., & York, B. M., Jr. (1987) *Prog. Clin. Biol. Res. 232*, 325–340.

Grimshaw, C. E., & Mathur, E. J. (1984) *Fed. Proc., Fed. Am. Soc. Exp. Biol. 43*, 2009.
Grimshaw, C. E., Shahbaz, M., & Jahangiri, G. (1988) *FASEB J. 2*, A1776.
Halder, A. B., & Crabbe, M. J. C. (1984) *Biochem. J. 219*, 33–39.
Hara, A., Deyashiki, Y., Nakayama, T., & Sawada, H. (1983) *Eur. J. Biochem. 133*, 207–214.
Håstein, T., & Velle, W. (1969) *Biochim. Biophys. Acta 178*, 1–10.
Hoffman, P. L., Wermuth, B., & von Wartburg, J.-P. (1980) *J. Neurochem. 35*, 354–366.
Humber, L. (1987) *Prog. Med. Chem. 24*, 299–343.
Jedziniak, J. A., & Kinoshita, J. H. (1971) *Invest. Ophthamol. 10*, 357–366.
Kador, P. F., & Sharpless, N. E. (1983) *Mol. Pharmacol. 24*, 521–531.
Kador, P. F., & Kinoshita, J. H. (1985) *Am. J. Med. 79* (*Suppl. 5A*), 8–12.
Kador, P. F., Kinoshita, J. H., Tung, W. H., & Chylack, L. T., Jr. (1980) *Invest. Ophthamol. Visual Sci. 19*, 980–982.
Kador, P. F., Shiono, T., & Kinoshita, J. H. (1983) *Invest. Ophthamol. Visual Sci. 24*, 267 (Suppl.).
Kador, P. F., Robison, W. G., Jr., & Kinoshita, J. H. (1985) *Annu. Rev. Pharmacol. Toxicol. 25*, 691–714.
Kinoshita, J. H. (1974) *Invest. Ophthamol. Visual Sci. 13*, 713–714.
Laemmli, U. K. (1970) *Nature* (*London*) *227*, 680–685.
Maragoudakis, M. E., Wasvary, J., Hankin, H., & Gargiulo, P. (1984) *Mol. Pharmacol. 25*, 425–430.
Mathur, E. J., & Grimshaw, C. E. (1986) *Arch. Biochem. Biophys. 247*, 321–327.
McKercher, S. M., Mathur, E. J., & Grimshaw, C. E. (1985) *Fed. Proc., Fed. Am. Soc. Exp. Biol. 44*, 472.
Morjana, N. A., & Flynn, T. G. (1989) *J. Biol. Chem. 264*, 2906–2911.
Morjana, N. A., Lyons, C., & Flynn, T. G. (1989) *J. Biol. Chem. 264*, 2912–2919.
Muller, P., Hockwin, O., & Ohrloff, C. (1985) *Ophthalmic Res. 17*, 115–119.
P-L Biochemicals (1961) Circular OR-18, P-L Biochemicals, Milwaukee, WI.
Poulsom, R. (1986) *Biochem. Pharmacol. 35*, 2955–2959.
Poulsom, R. (1987) *Prog. Clin. Biol. Res. 232*, 341–352.
Reed, J., & Kinzel, V. (1984) *Biochemistry 23*, 1357–1362.
Riddles, P. W., Blakeley, R. L., & Zerner, B. (1983) *Methods Enzymol. 91*, 49–60.
Rondeau, J.-M., Samama, J.-P., Samama, B., Barth, P., Moras, D., & Biellmann, J.-F. (1987) *J. Mol. Biol. 195*, 945–948.
Sander, E. G., & Jencks, W. P. (1968) *J. Am. Chem. Soc. 90*, 6154–6162.
Saravis, C. A., & Zamcheck, N. (1979) *J. Immunol. Methods 29*, 91–96.
Segel, I. H. (1975) in *Enzyme Kinetics*, pp 64–71, Wiley, New York.
Sheaff, C. M., & Doughty, C. C. (1976) *J. Biol. Chem. 251*, 2696–2702.
Sheys, G. H., & Doughty, C. C. (1971) *Biochim. Biophys. Acta 242*, 523–531.
Srivastava, S. K., Hair, G. A., & Das, B. (1985) *Proc. Natl. Acad. Sci. U.S.A. 82*, 7222–7226.
Stinson, R. A., & Holbrook, J. J. (1973) *Biochem. J. 131*, 719–728.
Tanimoto, T., Fukuda, H., & Kawamura, J. (1983) *Chem. Pharm. Bull. 31*, 2395–2403.
Turner, A. J., & Tipton, K. F. (1972) *Biochem. J. 130*, 765–772.
Turner, A. J., & Flynn, T. G. (1982) *Prog. Clin. Biol. Res. 114*, 401–402.
Wermuth, B. (1985) *Prog. Clin. Biol. Res. 174*, 209–230.
Wermuth, B., Bürgisser, H., Bohren, K., & von Wartburg, J.-P. (1982) *Eur. J. Biochem. 127*, 279–284.
Whittle, S. R., & Turner, A. J. (1981) *Biochim. Biophys. Acta 657*, 94–105.
Wilkinson, G. N. (1961) *Biochem. J. 80*, 324–332.
Williams, J. W., & Morrison, J. F. (1979) *Methods Enzymol. 63*, 437–467.
Willoughby, E. W., & Lambert, A. (1983) *Anal. Biochem. 130*, 353–358.
Winkler, F. K., D'Arcy, A., & Pirson, W. (1987) *J. Mol. Biol. 194*, 763.
Yang, J. T., Wu, C.-S. C., & Martinez, H. M. (1986) *Methods Enzymol. 130*, 208–269.